

# **A study of earthquake prediction by atmospheric precursors**

Zhonghao Shou

Darrell Harrington

Earthquake Prediction Center

*500E 63rd 19K, New York, NY 10021*

**<http://quake.exit.com>**

## **INTRODUCTION**

Whether or not earthquakes can be predicted has been argued for a long time. Fundamental to the reliable and precise prediction of earthquakes is the existence of a readily observable phenomenon, a precursor, with clearly identifiable links to a significant number of earthquakes. Numerous precursors have been proposed, including seismological, geodetic, hydrological, geochemical, electromagnetic, and animal behavioral, but despite a century of research, none has proven adequate to the task (Geller et al. 1997). In fact, when Nature invited authorities to discuss the issue of earthquake prediction, some contributors expressed doubt that earthquakes will ever be predictable (ref. Nature debates 1999). An examination of the arguments for and against predictability would be beyond the scope of this article. Nevertheless, the fact remains that none of the traditionally studied precursor candidates has led to successful predictions. In this article we describe the results of an extensive investigation into a potential link between earthquakes and atmospheric phenomena, a non-traditional precursor candidate.

A precursor based on atmospheric observations was first described in an ancient Chinese prediction as an "earthquake cloud", recorded in the Chronicle of Lon-De County, Ningxia, 380 years ago (Li, 1982). The correct prediction was remarkable because the predicted earthquake, the 7.0 Guyuan (36.5 N, 106.3 E), Ningxia earthquake on Oct. 25, 1622, was the only one of magnitude equal to or larger than 7 in Western China (<110 E) within 139 years from Jun.18, 1515 to Jul.20, 1654. Motivated by the success of this precursor, the author (Shou) has undertaken an ongoing qualitative study of images from weather satellites, in a search for the "earthquake cloud" or other related phenomena. The primary goals are to construct a sufficiently large dataset to determine whether there truly is a link between atmospheric phenomena and earthquakes, and if so, to develop a prediction methodology from it.

## **EARTHQUAKE CLOUDS**

The weather satellite image record is replete with examples of a tremendous variety of clouds. Careful study of this record has led us to believe that it includes clear examples of the so-called earthquake cloud. The key ingredients that enable identification of earthquake clouds amongst a jumble of meteorological features are their sudden appearance and large aspect ratio. Their characteristic length ranges from 150 to 900 km, and width from 20 to 45 km. Clouds typically develop over a time scale of several hours to a few seconds, the latter having been observed by eye over Southern California. Three empirical facts (Shou, 1999) enable the observer of an earthquake cloud to predict an earthquake. First, the cloud's tail generally points towards the epicenter. Second, the related earthquake's magnitude is a monotonic function of the cloud's mass. The greater

the mass, the stronger its associated earthquake. Third, the longest recorded delay between the appearance of an earthquake cloud and a subsequent earthquake is 78 days, and typical delays are about 30 days, although no clear correlation between delay times and observations has emerged. These facts reveal the three most important characteristics of an earthquake, from the perspective of public safety.

Fig. 1, a satellite image taken over Central Asia on Jan. 1, 1998, shows an example of an earthquake cloud. Based on this observation, on Jan. 5, 1998, the author predicted an earthquake of magnitude equal to or bigger than 6 in Afghanistan or its neighbors, in the region of 30-37N and 58-95E between Jan. 5 and Feb. 4, 1998. The prediction was certified by the United States Geological Survey (USGS) and was later validated by the magnitude 6.1 Ms Afghanistan earthquake at 37.07N and 70.09E, indicated by the tip of the arrow, on Feb. 4. Within the predicted time window, this earthquake was the only one equal to or bigger than magnitude 6 in the eastern half of the Northern Hemisphere. Fig. 2 shows a time series of images of an earthquake cloud originating in San Fernando, California on Jan. 3, 2001. On January 14, a pair of earthquakes of magnitude 4.1 and 4.3 occurred at 34.29N, 118.40W, San Fernando, exactly at the origin of the cloud. No other earthquakes of magnitude equal to or greater than 4 occurred in the area of 33.2~35.3N and 117.4~119.4W within 258 days from Dec. 25, 2000 to Sep. 8, 2001.

In total, Shou has identified more than 300 earthquake clouds, utilizing data from the GOES, Meteosat, GMS and IndoEx satellites, as well as visual observations. The processed satellite images are provided by Dundee University, University College London, Nottingham University, NOAA, Ohio State University, and Utah State

University. Of these cloud observations, 52 have been used to make predictions certified by the USGS and numerous others have been exhibited on our public website. Table 1 lists the predictions by earthquake clouds. For each prediction, a coarse window and a fine window are provided, in order to evaluate the precision of the technique. Each window is defined by a location range, a time range, and a magnitude range. Earthquake data are obtained from the National Earthquake Information Center (NEIC), USGS and the California Institute of Technology (Caltech) / USGS Seismic Network.

Of the 52 predictions, 35 or 67.3% of the coarse windows were correct; while 10 or 19.2% of the fine windows were correct. The set of 17 incorrect coarse predictions can be broken down as follows. In 6 cases, an earthquake of the predicted magnitude occurred within the specified area, but 8-30 days after the expiration of the time window. In 7 cases, an earthquake of the predicted magnitude occurred within the time window, but in the neighborhood of the predicted area. In 2 cases, multiple earthquakes did occur within the specified area and time, but the predicted magnitude was incorrect. In the other 2 cases, the earthquake was nearby, and either 2 days past the expiration of the time window, or smaller than the predicted magnitude.

## **STATISTICAL SIGNIFICANCE**

To evaluate whether the fraction of correct predictions is statistically significant, we applied the following calculation (Shou, 1999) to determine the probability of an earthquake occurring within a specified window. From a comprehensive earthquake database, select all earthquakes whose epicenters are within the predicted area and whose sizes are within the predicted magnitude range. Consider all intervals containing exactly

the same number of days as the predicted time span, within the time period of the database. Let A be the total number of such intervals. Let B be the number of such intervals in which a selected earthquake occurred. Then the probability of an earthquake occurring in the prediction windows is well-described by  $P=B/A$ . This quantity effectively represents the chance that a random choice of window of the same size as specified in the prediction would happen to coincide with an earthquake. The average probabilities for the coarse and fine windows over the entire set of predictions are 45.0% and 7.3%, respectively. The statistical significance of the prediction rate, however, is better expressed in the probability that a random guesser could make at least as many correct predictions as Shou did, given the same number of attempts, each with exactly the same probability of success as listed in Table 1. By averaging ten million simulations of the random guesser, we estimate his chance to equal or better Shou's success rate over the 52 earthquake cloud predictions to be .0017% or .080%, using coarse windows or fine windows, respectively. This result unequivocally demonstrates the statistical significance of the set of predictions, and suggests that there is a real physical link between the clouds and earthquakes.

Although the set of predictions is meaningful from a mathematical and scientific point of view, their utility to the general public would clearly benefit from a reduction in size of any of the three ranges. The magnitude range is currently the most reliable of the three components of the prediction window. It may be possible to reduce the range by adopting better quantitative techniques for evaluating the mass of an earthquake cloud. Nevertheless, its precision is ultimately limited by the precision of the magnitude reported by databases. Since reported magnitudes can vary by more than 1, and are sometimes

changed months to years after the earthquake, it would be more practical to attack a different component. Due to the lack of correlation with the time range, and the fact that its empirically-defined upper bound of 78 days is adequate for emergency planning purposes, working on the time range doesn't appear to be the most fruitful approach. The principal difficulty of this prediction method is in the area window - that the location of the cloud's initial appearance usually does not coincide with the epicenter. Presuming that the original source of the earthquake cloud is at or near the epicenter, knowledge of the local winds and of the delay between the physical process generating the cloud and its actual appearance, is required to pinpoint the epicenter.

## **GEOHERMAL ERUPTION**

In the search for a solution to this problem, we found a qualitatively different atmospheric phenomenon, which we denote geothermal eruption, or georruption. There are two key ingredients enabling the observer to distinguish this phenomenon in satellite weather images. First, georruption emerges as a sudden localized atmospheric heating or disappearance of cloud, often occurring at night. In some cases the size of the emergence is limited by the resolution of the freely-available satellite images, about 10 km. Since the warm region often grows rapidly after its onset, to as large as  $50 \times 50 \text{ km}^2$  after one hour, variation in the size of the emergence is as likely to be an artifact of the finite frequency of the images, which varies from hourly to bidaily, as to have any physical significance. The second characteristic is the persistence of the warm region despite the presence of moving clouds overlapping or in the vicinity. Typically the warm region

expands while its source point remains warm through the duration, which can be up to several days, but is normally less than one day.

Figure 3 shows a snapshot of several simultaneous geoeruptions in Taiwan on Jan. 30, 2000. Over the next 46 days, one or more earthquakes of magnitude greater than 4 occurred at each of the warm regions pinpointed (Table 2). Figure 4 shows a time series of images taken over the Eastern Mediterranean from 8:00 Feb. 23 to 2:00 Feb. 24, 2000. Based on these images, the author made a prediction certified by the USGS on Feb. 28, 2000 that there would be an M5 or two M4 earthquakes within a coarse window of latitude 36.5N to 38.5N, longitude 36E to 39E (shown in the figure) and 50 days from Feb. 28 to Apr. 18, and a fine window of latitude 37N to 37.8N, longitude 36.8-37.2E (too small to show) and 17 days from Mar. 25 to Apr. 10. The prediction was correct, as two earthquakes occurred at point B, well within the coarse window, at the edge of the fine window, and coinciding with a bulge in the geoeruption. No other earthquakes of magnitude equal to or bigger than 4 have occurred in the fine area window in more than 11 years since the beginning of the database on Jan.1, 1990. Within the fine time window, the predicted pair were the only earthquakes equal to or bigger than 4 in the region 29~44N, 31~48E, a region 637 times larger than the predicted area. Earthquakes also occurred later at points A and C, again coinciding with geoeruption features (Table 3).

To date, 142 geoeruptions have been identified, along with their subsequent earthquakes. A review of the dataset has revealed several empirical laws relating earthquakes to geoeruptions. First, the earthquake's epicenter often coincides with the point of emergence, although sometimes the source of the warm air is obscured by thick

clouds and the warm region appears first near the edge of the cloud bank. Second, the magnitude of the associated earthquake is a monotonically increasing function of the size and duration of the geoeruption. Third, the delay between a geoeruption and its associated earthquake ranges from 1 to 104 days, with an average of 30. Preliminary evidence suggests that the delay depends on at least two factors: the speed of development of the geoeruption, and its location on the earth's surface.

These observations have enabled Shou to make 10 earthquake predictions, of which 8 were correct. One erroneous prediction was the result of a clerical error, Shou having submitted the prediction after the earthquake already happened. In the other erroneous case, an earthquake of the predicted magnitude occurred within the predicted region, but was 38 after the expiration of the 30-day time window. This prediction was based on infrequent images and thus the point of emergence was difficult to pinpoint. Table 4 lists the geoeruption-based predictions and their probabilities, calculated in the same way as for earthquake clouds. The average probabilities for the coarse and fine windows are 33.9 % and 1.1% respectively, while the success are 80% and 10% respectively. Based on the simulation described above, the likelihood of a random guesser achieving an equal or better rate of success for the coarse predictions is 0.127%. The fine windows are often too small to obtain good statistics, as databases often contained no earthquakes of the specified magnitude within the specified area. We believe that since the geoeruption prediction methodology is not yet mature, refinement of the technique could lead to a significant improvement in precision and reliability.

## **DISCUSSION**

Clearly, the statistical significance of correct earthquake predictions based on earthquake clouds and geoeruptions indicates that they are connected in some way to earthquake epicenters. There are a limited number of reasonable hypotheses for this connection, the most obvious of which is that a significant quantity of hot gas, including water vapor, is expelled from the ground near an epicenter, days to months in advance of an earthquake. Depending on local meteorological conditions and the temperature and water content, this either locally heats the atmosphere above the epicenter, or condenses to form a cloud, after rising and possibly being carried by local winds some distance from the epicenter. There is plentiful observational evidence for the presence of high pressure superheated vapor at a hypocenter prior to an earthquake (Shi, Cai, and Gao, 1980; Yang, 1982; Glowacka and Nava, 1996; Lane and Waag, 1985; Shi and Cai, 1980; Zhang and Zhao, 1983). Yang (1982) reported that before the 7.3 Haicheng, China earthquake in 1975, the ice in a shaded portion of a frozen reservoir melted during a very cold winter. Lane and Waag (1985) reported that water spout erupted from as high as 115 feet above the valley floor at an estimated 400 cubic feet per second during the 7.3 Borah Peak, Idaho earthquake on October 28, 1983. Fig. 5 (China Academy of Architecture, 1986) shows damage to the ceiling of a structurally intact building due to the eruption of steam from underneath it during the 7.8 Tangshan earthquake on Jul. 28, 1976. Shi and Cai (1980) reported that carbon dioxide and other gases erupted violently from a dry well in Beijing prior to the Tangshan earthquake. Experimental work offers corroborating evidence of the tremendous temperatures and pressures (Spray, 1992; Swanson, 1992; Koch and Masch, 1992; Techmer, Ahrendt, and Weber, 1992). These may be sufficient to vaporize groundwater and force it to the surface. Laboratory experiments on a variety

of hydrated rocks suggest a mechanism by which the expulsion of vapor from the ground might be directly linked to the earthquake. Kirby and McCormick (1990) have shown that the yield strength of hydrated rocks is weakly dependent on temperature up to a critical temperature, past which the yield strength drops sharply as the water is vaporized. This dehydration process could potentially be a trigger for the earthquake.

## **SUMMARY**

We have observed two unusual atmospheric phenomena in weather satellite images. One is the sudden formation of a distinctive line-shaped cloud, historically known as an earthquake cloud. The other, which we denote *geoeruption*, is the sudden appearance and disappearance of a warm region tied to a particular location in spite of local meteorological conditions. Both phenomena are followed by an earthquake, typically a month afterwards. The earthquake's location is normally indicated by the cloud's tail, or the origin of the geoeruption. In an attempt to develop a prediction method based on this precursor, we have recorded 142 observations of geoeruptions, and more than 300 earthquake clouds. Shou has made 62 earthquake predictions based on these observations, with a success rate of 69.4%. We calculated probabilities of earthquakes occurring within the prediction windows by coincidence, and used these quantities to determine that the predictions are statistically significant. These preliminary results demonstrate that atmospheric precursors have the potential to indicate earthquakes with enough specificity and warning to benefit the general public. These results also raise the interesting possibility that hot vapor escapes from an earthquake's epicenter in sufficient quantity to be detected by satellites. An analysis of satellite data tailored towards

detecting this vapor might be the best approach to realizing the potential of atmospheric precursors.

## **Acknowledgments**

The authors gratefully acknowledge Wenying Shou for support, NOAA, Dundee University, UK and University College London for satellite images, the United States Geological Survey and its Southern California Data Center, California Institute of Technology, the Central Meteorological Bureau of Taiwan, Simin Li, Bogazici University of Turkey, and Resat Dengic for earthquake data, and China Academy of Building Research and China Academic Publishers for the photograph of earthquake damage.

## **References**

- 1 China Academy of Building Research (1986). *The Mammoth Tangshan Earthquake of 1976 Building Damage Photo Album*. 167 (China Academic Publishers. Beijing). In both Chinese and English.
- 2 Geller, R.J., D.D. Jackson, Y.Y. Kagan, and F. Mulargia (1997). Earthquakes cannot be predicted. *Science* **275**, 1616-1617.
- 3 Glowacka, E. and F. A. Nava, (1996). Major earthquakes in Mexicali Valley, Mexico, and fluid extraction at Cerro Prieto geothermal field. *Bulletin of the Seismological Society of America* **86**, No.1A, 93-105.

- 4 Kirby, S.H and J.W. McCormick (1990). Inelastic properties of rocks and minerals: strength and rheology. *Practical Handbook of Physical Properties of Rocks and Minerals* (ed. Carmichael, R.S) 177-200 (CRC Press, Boca Raton, Florida).
- 5 Koch, N. and L. Masch (1992). Formation of Alpine mylonites and pseudotachylytes at the base of the Silvretta nappe, Eastern Alps. *Tectonophysics* **204**, 289-306.
- 6 Lane, T. and C. Waag, (1985). Ground-water eruptions in the Chilly Buttes area, Central Idaho. *Special Publications* **91**, 19.
- 7 Li, D.J. (1982). *Earthquake Clouds*. 148-150 (Xue Lin Public Store, Shanghai). In Chinese.
- 8 Shi, H.X. and Z.H. Cai, (1980). Case examples of peculiar phenomena of subsurface fluid behavior observed in China preceding earthquakes. *Acta Seismologica Sinica* **2**, No.4, 425-429. In Chinese.
- 9 Shi, H. X., Z.H. Cai, and M.X. Gao, (1980). Anomalous migration of shallow groundwater and gases in the Beijing region and the 1976 Tangshan earthquake. *Acta Seismologica Sinica* **2**, No.1, 55-64. In Chinese.
- 10 Shou, Z. H. (1999). Earthquake clouds, a reliable precursor. *Science and Utopya* **64**, 53-57. In Turkish.
- 11 Spray, J.G. (1992). A physical basis for the frictional melting of some rock-forming minerals. *Tectonophysics* **204**, 205-221.
- 12 Swanson, M.T. (1992). Fault structure, wear mechanisms and rupture processes in pseudotachylyte generation. *Tectonophysics* **204**, 223-242.

- 13 Techmer, K.S., H. Ahrendt, and K. Weber (1992). The development of pseudotachylyte in the Ivrea-Verbano zone of the Italian Alps. *Tectonophysics* **204**, 307-322.
- 14 Yang, C.S., (1982). Temporal and spatial distribution of anomalous ground water changes before the 1975 Haicheng earthquake. *Acta Seismologica Sinica* **4**, No.1, 84-89. In Chinese.
- 15 Zhang, D.Y. and G.M. Zhao, (1983). Anomalous variations in oil wells distributed in the Bohai bay oil field before and after the Tangshan earthquake of 1976. *Acta Seismologica Sinica* **5**, No.3, 360-369. In Chinese.

Correspondence and requests for materials should be addressed to

Zhonghao Shou

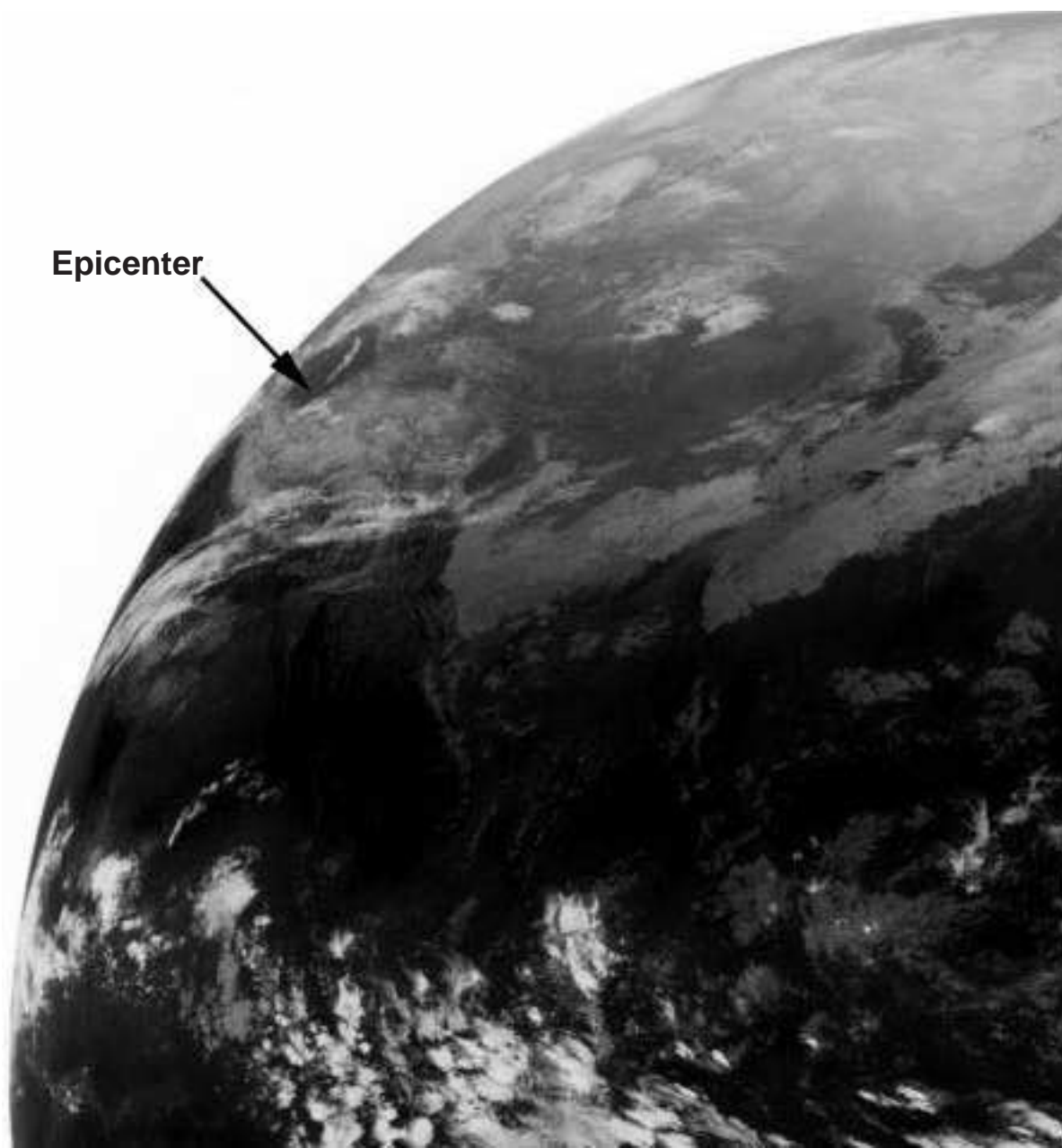
500E 63rd 19K

New York, NY 10021

email: [zhonghao\\_shou@yahoo.com](mailto:zhonghao_shou@yahoo.com)

**Tel: (212) 829-7196**

**Fax:**



Epicenter

Fig. 1 Afghanistan earthquake cloud

This image from the GMS satellite was provided by University College London \*. At about 7:32 Jan.1, 1998, a hole with a line-shaped cloud inside appeared in a large weather cloud. The line-shaped cloud disappeared at about 16:25. Shou predicted an earthquake of magnitude equal to or larger than 6 in Afghanistan and its neighbors, 25~41N and 53~105E from Jan. 5 to Feb. 18, and most likely within 30~37N and 58~95E, from Jan.5 to Feb.4, 1998 to the United States Geological Survey. The 6.1 Afghanistan earthquake at 37.075N, 70.089E, marked by the tip of the arrow, on Feb. 4 proved the prediction correct.

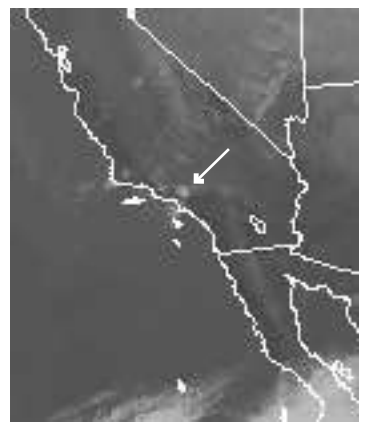
\* <http://weather.cs.ucl.ac.uk/Weather/gms/jpg/ir1/4km/>



20010102 22:30



20010102 23:00



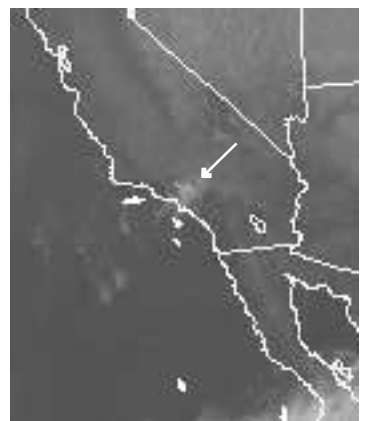
20010103 0:00



20010103 1:00



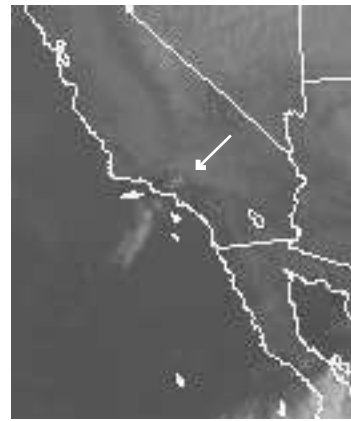
20010103 2:00



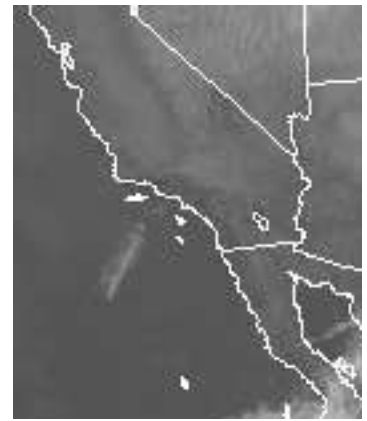
20010103 3:00



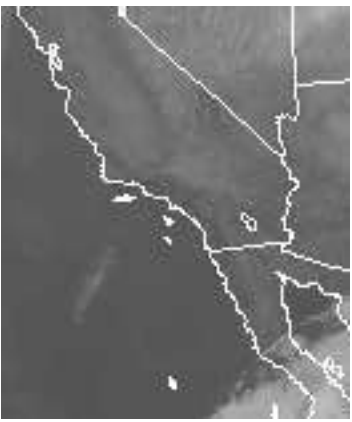
20010103 4:00



20010103 5:00



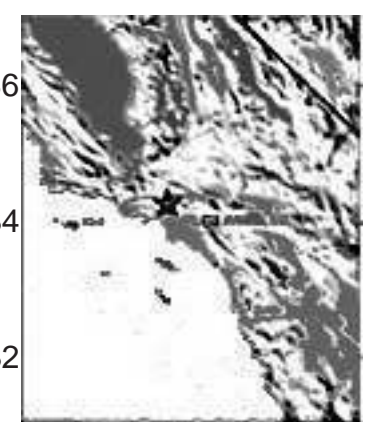
20010103 6:00



20010103 7:00



20010103 8:00



-120 -118 -116

## Fig. 2 San Fernando earthquake cloud

This figure shows a time series of GOES10 images of Southern California, provided by NOAA \*. A small cloud emerged in a cloudless sky over San Fernando at 23:00 Jan. 2, 2001 and another appeared at 1:00 Jan. 3. The clouds grew towards the west and southwest, and eventually moved away from their origin, which is marked by a white arrow. One disappeared at 4:00 and the other before 8:00. On Jan. 14, an M4.3 and an M4.1 earthquake occurred at 34.29N, 118.40W, San Fernando, exactly at the origin of the clouds. The final frame shows the USGS report on the M4.3 quake, which marks its location with a star.

\* <http://www.goes.noaa.gov>

Table 1. Predictions by Earthquake Clouds vs. Earthquakes

Predictions by Earthquake Clouds						Earthquakes									
No	Date	C	Time Span F LT	Area Latitude, Longitude	Mag.	Date UTC	Time	Lat.	Lon.	Mag.	Check T A M			Pro. %	
1	940213	C	0213~0310	Around Pas.	4~5.5	0225	12:59	34.36	-118.48	4.0	M	v	v	v	13.8
		F	0218~0305												
2	940305	C	0305~0330	Mex., S Cal.	5.5~6.8	0314	20:51	15.99	-92.43	6.3	A	v	v	v	32.7
		F	0310~0324												
3	940315	C	0315~0409	50~150km to Pas.	4~5.5	0320	21:20	34.23	-118.48	5.2	M	v	v	v	26.8
		F	0320~0404												
4	940315	C	0321~0415	30~45, 65~80	5~6.8	0501	12:00	36.90	67.16	6.1	A	x	v	v	64.9
		F	0321~0402	33~39, 68~74	6~6.8								x	x	v
5	940330	C	0330~0424	Cal.	5~7	0406	19:01	34.19	-117.10	4.8	M	v	v	v	27.1
		F	0331~0416	NW from Pas.	5.5~6.5								v	x	x
6	940423	C	0423~0518	N Mex., S Cal.	>=4	0512	0:22	25.07	-109.28	5.0	A	v	v	v	73.1
		F	0428~0501 0506~0508	<120km to Pas.	4.5~5.5								x	x	v
7	940603	C	0603~0628	S Cal.	3.7~5.5	0615	5:59	34.31	-118.40	4.1	M	v	v	v	79.6
		F	0616~0618	NW, 30~100km to Pas.	4~5								x	v	v
8	940910	C	0910~0925	20~50, 0~75	>=6	1025	0:54	36.36	70.96	6.0	A	x	v	v	20
		F	0910~0913	Mid-east	>=7								x	v	x
9	940916	C	0916~1011	Japan ~ Ale. with 500km	>=5	1004	13:22	43.77	147.32	7.9	A	v	v	v	99.9
		F	0916~1003	Kamchatka ~ Ale.	>=6								v	x	v
10	941008	C	1018~1112	USA	>=5	1027	17:45	43.52	-127.43	6.0	A	v	v	v	48.1
		F	1019~1025	34~37, -114~-105	>=6								x	x	v
11	950307	C	0307~0401	Mex., S Cal.	>=4	0326	14:32	31.26	-114.35	4.2	M	v	v	v	100
		F	0308~0323	32~34, -119~-117	>=5								x	x	x
12	950630	C	0630~0720	S Cal.	>=5	0630	11:58	24.69	-110.23	6.1	A	v	x	v	8.9
		F		NW, 60~80km to Pas.	>=6									x	v
13	951011	C	1011~1105	Cal.	>=5	1021	2:39	16.84	-93.47	6.6	A	v	x	v	27.1
		F	1017~1027	Near San Francisco	6~7								v	x	v
14	960510	C	0510~0530	S Cal.	3.7~5.3	0521	20:50	37.36	-121.72	4.6	A	v	x	v	31.6
		F	0512~0523	NW, 25~75km to Pas.	4~4.8								v	x	v
15	961025	C	1025~1119	S Cal.	>=4.5	1127	20:17	36.08	-117.65	5.3	M	x	v	v	28.5
		F		34~35, -121~-118										x	
16	961125	C	1125~1220	Mex. ~ Peru	>=6	1231	12:41	15.83	-92.97	6.0	A	x	v	v	44.8
		F	1125~1210	15~22, -105~-95										x	x
17	961204	C	1204~1229	S Cal., N Mex. >30N	4~5.3	1217	4:03	36.08	-117.65	3.9	A	v	v	v	48
		F	1207~1222	32~35N										v	x
18	961206	C	1206~0105	Mex.	>=4.5	1208	23:52	14.99	-94.02	4.9	A	v	v	v	98.1
		F	1212~1226	18~29N	6~7									x	x
19	970306	C	0306~0405	N China >35N	>=6	0405	23:46	39.51	76.87	5.8	A	v	v	v	12.8
		F		105~115E			0406	4:36	39.54	77.0	5.7	A		x	
20	970424	C	0424~0610	S Cal.	>=4	0426	10:37	34.37	-118.67	5.1	M	v	v	v	79.4
		F	0427~0514	<36, <-118			0427	11:09	34.38	-118.65	4.9	M	v	v	
21	970427	C	0427~0611	S Cal.	3.7~5.3	0506	19:12	35.45	-118.43	4.5	M	v	v	v	93.7
		F	0429~0520	<119W										v	v
22	970508	C	0508~0608	S Cal.	4~5.3	0524	4:36	35.80	-117.64	4.0	M	v	v	v	63.4
		F	0508~0525	<118.5W										v	v

23	970528	C	0528~0712	Turkey & Med. $\geq 15E$	$\geq 5.5$	0601	12:54	36.16	31.30	5.6	M	v	v	v	35.6
		F		25~35E									v		14.7
24	970718	C	0719~0809	S Cal.	$\geq 4$	0726	3:14	33.40	-116.35	4.9	M	v	v	v	50.2
		F		33~35, -117.8~-115.8 or 34~35, -119~-118.4									v		35.5
25	970804	C	0804~0828	S Cal.	$\geq 4$	0821	16:11	38.57	-118.5	4.5	A	v	x	v	34.
		F	0805~0820	NW, 20~80km to Pas.	4.7~5.3		16:56	38.56	-118.49	4.4	A	x	x	x	1.9
26	980105	C	0105~0218	25~41, 53~105	$\geq 6$	0204	14:33	37.07	70.09	5.9	A	v	v	v	44.1
		F	0105~0204	30~37, 58~95									v	v	20.8
27	980106	C	0106~0220	Mex.	$\geq 5$	0203	3:02	15.88	-96.30	6.4	A	v	v	v	79.5
		F	0110~0129	20~25, -105~-100	$\geq 5.5$								x	x	0
28	980309	C	0309~0423	15~30, <-150	$\geq 4$	0507	23:15	19.22	-155.51	4.3	A	x	v	v	31.7
		F	0312~0401		$\geq 5$								x	x	3
29	980406	C	0406~0522	Mex., Cal., <34N	$\geq 4.5$	0425	11:19	17.68	-94.19	5.0	A	v	v	v	99.3
		F	0409~0501	27~32N	4.9~5.3								v	x	3.7
30	980724	C	0724~0902	34~39, -119~-117	4~5.5	0801	6:01	37.58	-118.78	4.2	M	v	v	v	54.9
		F	0724~0813	35~38.5N	4.3~5.2								v	v	18.7
31	981123	C	1123~0109	Cal. <39N	$\geq 4.5$	1212	1:41	37.51	-116.29	4.4	A	v	v	v	72.3
		F	1124~1218	35~37.7, -119~-116	$\geq 5.5$								v	v	2.4
32	981228	C	1228~0213	33~39, -120~-116	4.2~5.4	0127	10:44	36.81	-115.99	4.6	A	v	v	v	69.9
		F	0101~0120	35~37.7N, -119~-116	4.6~5.1								x	v	9.9
33	990222	C	0222~0408	20~38, 50~100	$\geq 5.5$	0304	5:38	28.34	57.19	6.5	A	v	v	v	61.8
		F	0305~0330	29~35, 68~72	$\geq 6$								x	x	1.3
34	990402	C	0402~0520	24~34, -118~-108	4~5.2	0428	19:08	30.30	-115.54	4.4	A	v	v	v	77.6
		F	0406~0426	30~33, -117~-112	4.5~4.9		19:34	30:25	-115.61	4.3	A	x	v	v	4.3
35	990412	C	0412~0529	34~39, <-116	$\geq 4$	0514	7:54	34.06	-116.37	4.7	A	v	v	v	83.1
		F	0412~0430	<37, <-119	$\geq 5$								x	x	0.9
36	990505	C	0505~0621	27~33, -117~-113	$\geq 4$	0601	15:18	32.37	-115.24	5.0	A	v	v	v	40
		F	0506~0526	29.5~30.5, -115.5~-114.5	$\geq 4.8$								x	x	0
37	990517	C	0517~0704	Mex. <29N	$\geq 5$	0615	20:42	18.39	-97.44	6.7	A	v	v	v	79.5
		F	0525~0615	22~25, -106~-104	$\geq 6$								v	x	0
38	990609	C	0609~0725	35~39, -120~-116	4~5.3	0711	18:20	35.73	-118.48	4.4	M	v	v	v	61.9
		F	0615~0705	37~38.7, -119~-118	4.6~4.8								x	x	3
39	990726	C	0726~0910	36~42, 113~117	$\geq 5$	0817	10:41	29.41	105.61	4.8	A	v	x	v	4.7
		F	0812~0830	40.5~41.5, 114~115	$\geq 6$								v	x	0
40	991028	C	1028~1214	30~33, -117~-115	$\geq 4.3$	1114	14:20	34.84	-116.41	4.5	M	v	x	v	15.7
		F	1101~1120	32~33, -116.5~-115.5	$\geq 4.6$								v	x	0
41	991025	C	1025~1114	30~40, 51~58	$\geq 6$	1112	16:57	40.76	31.16	6.9	A	v	x	v	1.5
		F			$\geq 6.5$									v	1.5
42	991227	C	1227~0210	Indian Ocean >20S	$\geq 7$	0209	18:40	-27.62	65.72	5.0	A	v	v	x	0
		F	1227~0116	-28~-25, 67~70	$\geq 7.2$	0209	18:40	-27.69	65.71	5.0	A	x	x	x	0
						0210	14:18	-27.58	65.73	5.4	A				
						0210	14:18	-27.66	65.68	5.4	A				
						0210	23:00	-27.58	65.78	5.3	A				
						0210	23:00	-27.63	65.76	5.4	A				
43	000131	C	0131~0311	Iran <30, 58~68	$\geq 4.5$	0217	9:44	29.58	67.12	4.6	A	v	v	v	45.8
		F	0205~0225	61~63E	$\geq 5$								v	x	2
44	000218	C	0218~0310	Iran <32, 57~58	$\geq 4.5$	0229	17:16	28.25	57.14	4.5	A	v	v	v	18.1
		F	0218~0225	28~31N	$\geq 5$								x	v	1.3
45	000228	C	0228~0413	31~35, -116.5~-115	$\geq 4.5$	0409	10:48	32.69	-115.39	4.3	M	v	v	v	21.6
		F	0304~0324	32.2~32.5, -115.5~-115.1	$\geq 5$								x	v	0
46	000705	C	0705~0821	Japan <34, <142.5	$\geq 6$	0730	12:25	33.9	139.38	6.4	A	v	v	v	32.2
		F	0705~0725	29~32, 130~132.5	$\geq 6.6$								x	x	0.5
47	000714	C	0714~0807	Mex. Cal. 32~39, <-114	$\geq 5$	0809	11:41	18.2	-102.48	6.4	A	x	x	v	20.7

		F		35~36.8, -119~-117	>=7									x	x	x	0
48	010321	C	0321~0505	Cal. >38N	>=4.5	0322	21:22	40.48	-126.18	4.6	A	v	v	v	v	v	45.2
		F	0321~0401	39~40, -123.3~-122.7	>=5.5									v	x	x	0
49	010405	C	0405~0522	36~43, 25~36	>=5.5	0501	6:00	35.7	27.5	4.9	A	v	x	x	x	x	12.4
		F	0405~0410		>=6.3									x		x	0.3
50	010731	C	0731~0929	USA, Can. 42~53, <-112	>=6	0914	4:45	48.69	-128.71	5.8	A	v	v	v	v	v	16.4
		F	0820~0927	51.2~52.2, -115.5~-114.5	>=6.5									v	x	x	0
51	010806	C	0806~1021	21~25, 68~73	>=6	0920	13:24	23.57	70.28	4.7	A	v	v	x	x	x	0
		F	0810~0910	23.1~23.7, 70~70.6	>=6.5	0921	2:40	23.47	70.07	4.7	A	x	v	x	x	x	0
52	010808	C	0808~1002	32~33.5, -117~-115.2	>=4	1031	7:56	33.51	-116.51	5.0	A	x	v	v	v	v	8.4
		F	0815~0905	32.5~32.7, -116.4~-116.2	>=4.5									x	x	v	0

Notes:

1. Column 3, C: coarse. F: fine. Column 4, LT: Los Angeles Times. Column 5, latitude data are before longitude data. Ale.: Aleutian. Cal.: California. Can.: Canada. Med.: Mediterranean. Mex.: Mexico. Pas.: Pasadena. Column 6 and 11, Mag.: magnitude. Column 9, Lat.: latitude. Column 10, Lon.: longitude. Column 12, A: an average of magnitudes by the data of the NEIC, USGS. M: ML from the Caltech/ USGS Seismic Network. Column 13~15, T: time, A: area, M: magnitude, v: correct, x: incorrect. Column 16, Pro.: probability.
2. We estimate the error in our calculation of latitude and longitude to be 0.1°. Database errors are quoted as at least 0.1° and 0.1 ML, although typical variations between databases are often much greater.
3. The distance between Pasadena (34.133, -118.125) and the predicted epicenter of No.1, No.3, and No.7 is 39.0, 33.4, and 32.0 km respectively.
4. The earthquake data for prediction No. 23 came from Bogazici University of Turkey.

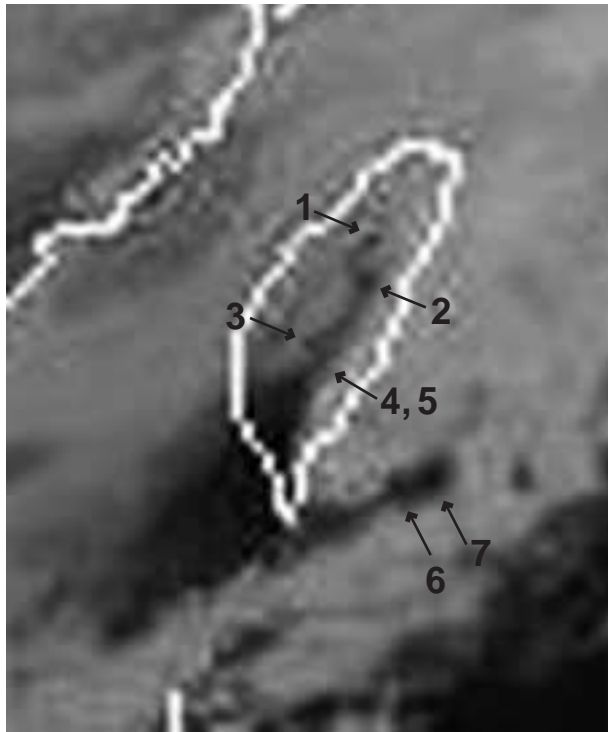


### Fig. 3 Taiwan geothermal eruption

This image from the GMS satellite over Taiwan at 3:00 Jan. 30, 2000 was provided by Dundee University, UK \*. Several dark spots, indicating warm regions, appear in the midst of cloud cover. Their unusual appearance leads us to believe that they were not weather-related, but instead were geothermal eruptions. Over the next 45 days, a series of 8 earthquakes occurred at exactly the locations of the dark spots, as shown by the arrows. The earthquake data are shown in Table 3. The mottled appearance of parts of the image is a result of magnifying a small jpeg file.

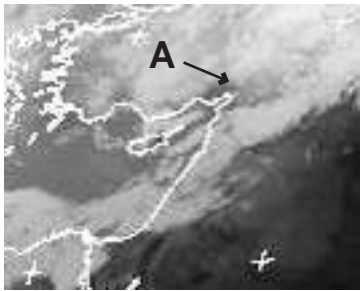
\* <http://www.sat.dundee.ac.uk/pdus/JI>

Table 2 Taiwan Georptions vs. Earthquakes

Georptions					Earthquakes							
Date UTC	Time	P	Lat. N	Lon. E	Date UTC	Time	Lat. N	Lon. E	Mag. ML	mb	Dep. Km	S
20000130	3:00	1	24.0	121.2	000130	20:21	23.90	121.31	4.8	4.1	33	U
							23.90	121.31	4.8		7.5	T
		2	23.5	120.7	000131	2:57	23.51	120.48	4.2		4.7	T
		3	24.4	121.1	000131	21:11	24.37	120.9	4.6		4.2	T
					000216	19:48	24.35	120.8	4.0		7.4	T
		4	23.2	120.7	000215	21:33	23.35	120.93		5.3	33	U
							23.33	120.75	5.6		21.1	T
		5	23.2	120.7	000216	0:33	23.33	120.75	4.5		13.4	T
		6	22.2	121.4	000226	8:23	22.24	121.37		4.1	33	U
		7	22.2	121.8	000316	0:37	22.06	121.62	5.0	4.8	33	U

Note:

1. P: point number. Lat.: latitude. Lon.: longitude. Mag.: magnitude. Dep.: depth. S: source. U: the USGS. T: the Central Meteorological Bureau of Taiwan, received by Journalist Simin Li.
2. The latitudes and longitudes of the georptions were calculated directly from the image, and have an uncertainty of  $0.2^\circ$ .
3. The average latitude and longitude absolute errors between the earthquake data and the georruption data are  $0.09^\circ$  and  $0.15^\circ$ , respectively.



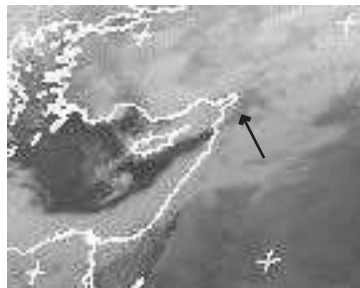
20000223 8:00



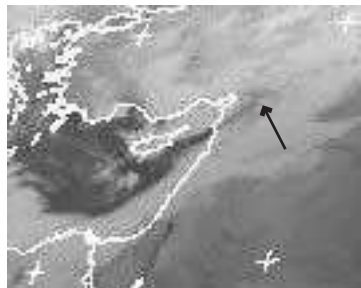
20000223 14:00



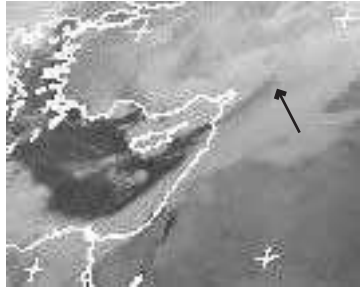
20000223 15:00



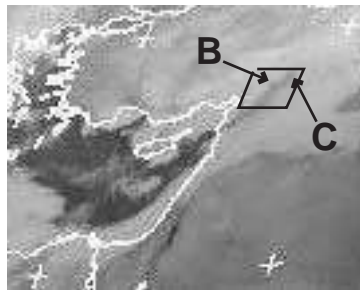
20000223 17:00



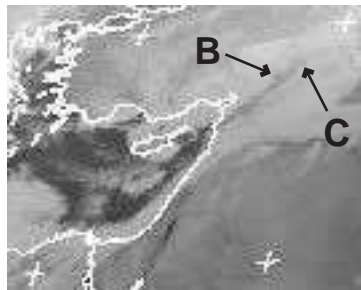
20000223 18:00



20000223 19:30



20000223 21:00



20000223 22:00



20000224 2:00

#### Fig. 4 Turkey geothermal eruption

This series of IndoEx satellite images of the Eastern Mediterranean was provided by Dundee University \*. A geotherm had occurred in Turkey at Point A (37N, 36.1E) at 8:00 Feb. 23, 2000, and disappeared at 15:00. Meanwhile, another warm spot appeared at Point X and grew toward the northeast. Two small bulges appeared at Points B (37.8N, 37.2E) and C (38.2N, 38E) at 21:00. Based on the feature at Point B. Shou predicted an earthquake to the USGS. The coarse area window of the prediction is shown by the black rectangle and the fine area window coincides with Point B. Two earthquakes of magnitude 4.2 and 4.4 occurred at Point B on April 2, 2000, 39 days later. Earthquakes also occurred at A on May 12 and C on May 7. All data are shown in Table 3.

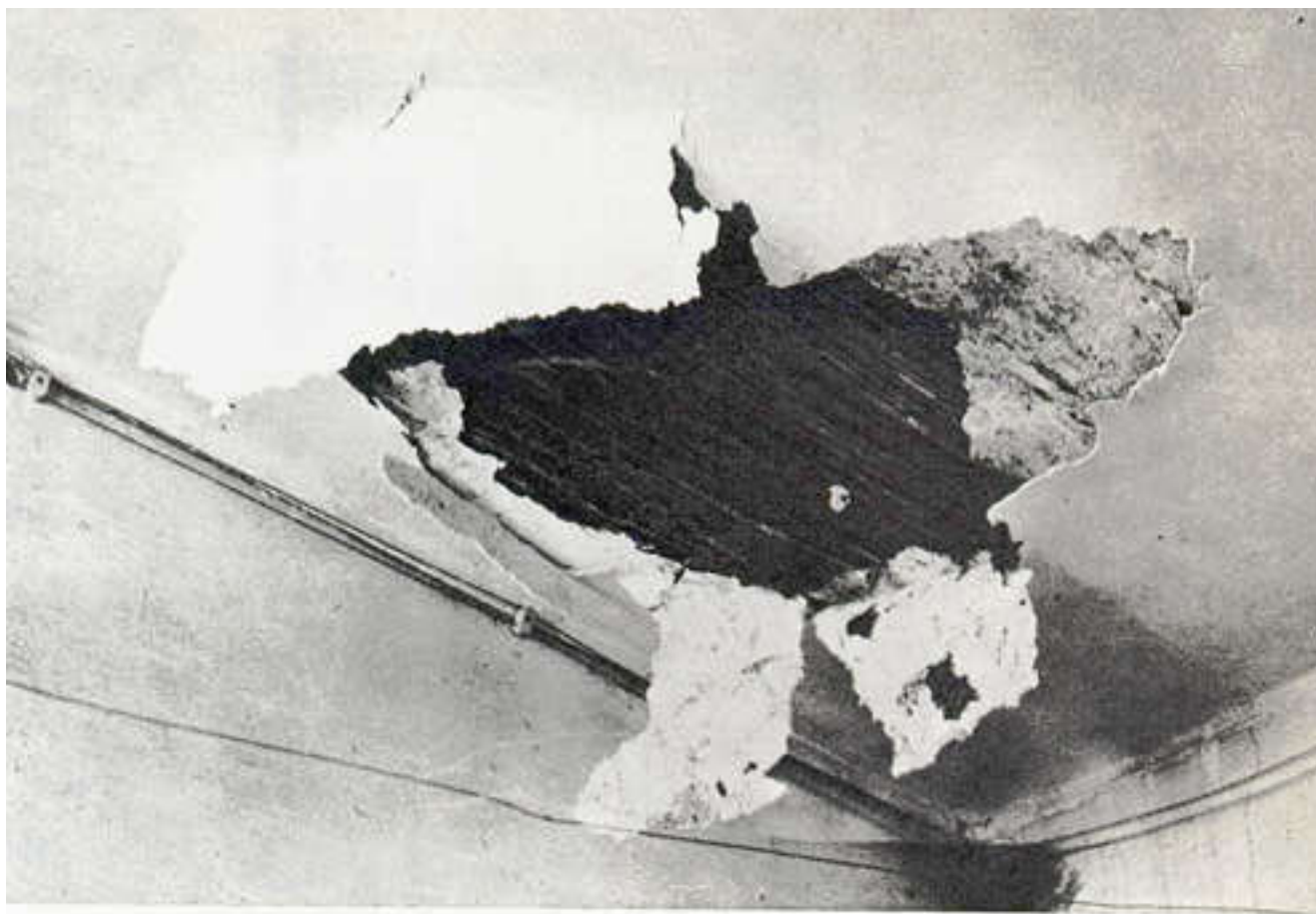
\* <http://www.sat.dundee.ac.uk/pdus/XI>

Table 3 Turkey Georuptions vs. Earthquakes

Georuptions					Earthquakes					
Date UTC	Time	P	Lat. N	Lon. E	Date UTC	Time	Lat. N	Lon. E	Mag. mb	Dep. Km
20000223	8:00	A	37.0	36.1	000512	3:01	37.05	36.08	4.7	10
	21:00	B	37.8	37.2	000402	11:41	37.57	37.19	4.4	9
					000402	17:26	37.65	37.23	4.2	9
	22:00	C	38.2	38.0	000507	9:08	38.18	38.75	4.2	1.6
					000507	23:10	38.16	38.78	4.5	5.4

Note:

Besides notes in Table 2, the earthquake data are from the USGS, and the average latitude and longitude absolute errors between the earthquake data and the georuption data are 0.10° and 0.32°, respectively.



7-17 丰南县宜庄公社一平房内喷沙冒水，冲破了房屋顶棚(10度区)。

In the area of intensity 10, sand boiling and water spouting occurred to a house in Yizhuang Commune in Fengnan County and spoiled the ceiling.

Fig. 5 Tangshan earthquake damage

The image shows damage in the roof of a building caused by steam erupting from the ground during the 1976 Tangshan earthquake. Similar phenomena occurred during other large earthquakes such as the 6.8 and the 7.2 Xingtai, Hebei, China quakes on March 8 and March 22, 1966, and the 7.3 Haicheng, Liaoning, China quake on Feb. 4, 1975.

Photo ©China Academic Publishers.

Table 4. Predictions by Georruption vs. Earthquakes

Predictions by Georruption						Earthquakes									
No	Date	C F	Time Span LT	Area Latitude, Longitude	Mag.	Date UTC	Time	Lat.	Lon.	Mag.	A	Check T A M			Pro %
1	990825	C	0825~1003	N Cal. >38,<-122	>=5.5	0818	1:06	37.91	-122.69	4.8	A	x	v	x	6
		F	0825~0910	40~40.5,-124.5~-124	>=6.3								x	x	x
2	000228	C	0228~0418	36.5~38.5,36~39	1M5/2M4	0402	11:41	37.57	37.19	4.2	A	v	v	v	6.8
		F	0325~0410	37~37.8,36.8~37.2	>=5.5	0402	17:26	37.65	37.23	4.4	A	v	v	x	0
3	000322	C	0322~0505	35.8~40,-120~-117	>=4	0328	15:16	36.02	-117.87	4.3	A	v	v	v	37.7
		F	0323~0415	35.8~36.3,-118~-117.5	>=4.5								v	v	v
4	000421	C	0421~0604	34~35.5,-119.5~-118	>=4	0518	9:41	35.10	-118.31	3.9	M	v	v	v	24.3
		F	0425~0515	34.4~34.9,-118.7~-118.3	>=4.7								x	v	x
5	000422	C	0422~0605	33.5~37,-118~-115	>=4	0523	4:42	36.32	-118.07	4.0	M	v	v	v	60.3
		F	0425~0515	34.5~35,-117.8~116	>=5								x	x	x
6	000626	C	0629~0820	Japan, <37	>=6	0701	7:01	34.22	139.13	6.1	A	v	v	v	37.7
		F	0629~0710	34~35.2,139.1~139.7	>=7								v	v	x
7	010320	C	0320~0504	N Cal., -126~-122	>=4.5	0420	5:19	40.68	-125.32	4.4	A	v	v	v	29.3
		F	0320~0401	39~40.5, -126~-124	>=5.5								x	v	x
8	010426	C	0426~0615	USA~Can,38~54,<-120	1M5/2M4	0502	2:05	49.91	-130.15	4.9	A	v	v	v	71.7
		F	0428~0518	44~50, <-122	>=5.5								v	v	x
9	010509	C	0509~0609	26~42, <-112	>=5	0717	12:07	36.01	-117.86	4.9	A	x	v	v	46.7
		F	0509~0515	33~36, -120~-117	>=6								x	v	x
10	010403	C	0403~0702	36.3~37.2, -121.5~-120	>=4	0702	17:33	36.70	-121.33	4.1	M	v	v	v	18.8
		F	0410~0510	Holister, Cal.	4.3~4.8								x	v	v

Notes:

Besides notes in Table 1, Column 6, 1M5/2M4: one quake of magnitude 5~5.9 or two 4~4.9.